Efficient Photoluminescence of Mn^{2+} Ions in MnS/ZnS Core/Shell Quantum Dots

Jinju Zheng,[†,‡] Xi Yuan,[†,‡] Micho Ikezawa,[§] Pengtao Jing,[†,‡] Xueyan Liu,[†] Zhuhong Zheng,[†] Xianggui Kong,[†] Jialong Zhao,*[,†] and Yasuaki Masumoto*[,§]

Key Laboratory of Excited State Processes, Changchun Institute of Optics, Fine Mechanics and Physics, Chinese Academy of Sciences, 3888 Eastern South Lake Road, Changchun 130033, China, Graduate School of Chinese Academy of Sciences, Beijing 100039, China, and Institute of Physics, University of Tsukuba, Tsukuba, Ibaraki 305-8571, Japan

Received: July 7, 2009; Revised Manuscript Received: August 19, 2009

We have studied the mechanism of photoluminescence (PL) from MnS/ZnS core/shell quantum dots (QDs) synthesized via hot solution phase chemistry using a nucleation−doping strategy. Efficient PL of the Mn^{2+} ions with a quantum yield (QY) of over 35% is demonstrated in the resulting QDs coated with a thick ZnS shell on the MnS core. The MnS/ZnS core/shell QDs with a thick shell exhibit PL enhancement with increasing temperature in the range between 140 and 300 K, resulting from the thermal activation of charge carriers localized at the interface between the MnS core and the ZnS shell. The PL decays of the Mn^{2+} ions in the core/shell QDs consist of three exponential components with time constants on the scales of 1−2 ms, hundreds of μs, and tens of μs. Surprisingly, the PL lifetimes of Mn^{2+} ions show a very weak dependence on the shell thickness, which is clearly different from that of the PL QY of the QDs. The experimental results indicate that the mechanism for improving the PL QY in MnS/ZnS QDs can be understood in terms of a significantly enhanced energy transfer from the ZnS shell to Mn^{2+} ions and a slightly decreased nonradiative relaxation rate from Mn^{2+} ions to surface states/traps of the ZnS shell by the surface passivation of the QDs with a thick ZnS shell.

Introduction

Mn-doped ZnS quantum dots (QDs), also called ZnS:Mn d-dots, with the large absorption cross sections of the ZnS hosts and rapid energy transfer from the host to the dopants are expected to yield highly efficient photoluminescence (PL) of Mn^{2+} ions.[1−6] Therefore, these ZnS:Mn d-dots have promising applications in optoelectronic devices[1,2] as well as in biomedical labeling.[3,4] The earliest report about ZnS:Mn d-dots was given in 1983,[5] although a dramatically increased interest in doped QDs was stimulated by Bhargava et al., who claimed in 1994 that the PL lifetime of Mn^{2+} ions in ZnS:Mn d-dots was 5 orders of magnitude shorter (∼20 ns) than that in bulk and the PL quantum yield (QY) was greater.[6] Since then, the PL properties of ZnS:Mn d-dots have been widely studied.[7−9] In particular, recent studies showed that the PL of Mn^{2+} ions in groups II−VI semiconductor QDs was also dependent on the structure of the QDs and the doping position of Mn^{2+} ions in the host dots.[10−12] For instance, compared to CdS:Mn/ZnS core/shell QDs, ZnS/CdS:Mn/ZnS quantum well (QW) QDs exhibit a significant enhancement in PL intensity perhaps due to suppressed nonradiative relaxation.[11] Therefore, the mechanism of the radiative and nonradiative relaxation processes for the doped QDs is needed to be well-understood for further improvement of the PL QY and photo/thermal stability by adjusting the structure of the QDs and the doping position of Mn^{2+} ions in the host dots.

In general, it is difficult to precisely control the placement of the dopant ions at a desired radial position in the host dots using the traditional synthetic approaches, which are generally based on a reaction system with both dopant ions and competitive host ions.[7−9,13−15] Recently, Peng's group[16] reported a simple synthesis of radial-position-controlled doping of QDs by the growth of a ZnSe shell on the MnSe core using a nucleation−doping strategy. The obtained QDs can also be called ZnSe:Mn d-dots because of their similar emission properties[16] or MnSe/ZnSe:Mn/ZnSe spherical QW QDs from the structural viewpoint. The reliable synthesis of QW structures realizes the position-controlled doping of Mn^{2+} ions in semiconductor nanostructures, resulting in an improvement in the PL QY of Mn^{2+} ions and the photo/thermal stability of the QDs. As we know, ZnS:Mn d-dots are a typical kind of doped semiconductor nanostructures. However, no report has been given yet by now about the optical properties of such ZnS:Mn d-dots prepared by the growth of a ZnS shell on the MnS core using a nucleation−doping strategy.

The surface passivation by growing an inorganic shell on Mn-doped groups II−VI semiconductor QDs has been successfully used to improve the PL QY and photo/thermal stability of Mn-doped QDs. Enhanced PL of Mn-doped core/shell QDs was observed in ZnS:Mn/ZnS,[17,18] ZnS:Mn/ZnO,[19] and CdS:Mn/ZnS.[20,21] Cao and co-workers[18] observed the 7 times enhancement of PL intensity after the formation of a ZnS shell on ZnS:Mn d-dots. Recently, Lin et al.[17] reported a 30% enhancement in the PL intensity and a somewhat increase in the PL lifetime in ZnS:Mn/ZnS core/shell QDs with respect to those of bare ZnS:Mn d-dots. Further, compared to the ZnSe/ZnMnS core/shell QDs, ZnSe/ZnMnS/ZnS QDs with the structure of a QW exhibited a more significant improvement in the PL QY and stability of the QDs.[1,4] These studies have consistently shown

* To whom correspondence should be addressed. Phone: +86-431-86176029 (J.Z.), +81-29-8534248 (Y.M.). E-mail: zhaojl@ciomp.ac.cn (J.Z.), shoichi@sakura.cc.tsukuba.ac.jp (Y.M.).

† Changchun Institute of Optics, Fine Mechanics and Physics, Chinese Academy of Sciences.

‡ Graduate School of Chinese Academy of Sciences.

§ Institute of Physics, University of Tsukuba.

10.1021/jp906390y CCC: $40.75
Published on Web 09/08/2009

that the passivation of ZnS or ZnO shells on Mn-doped groups II−VI semiconductor nanostructures can efficiently block the nonradiative recombination centers, leading to the significant improvement of the PL QY. However, the shell thickness dependence of the PL properties in Mn-doped ZnS QDs has not been understood in detail yet.

In this work, we report the synthesis of high-quality MnS/ZnS core/shell QDs with a Mn-emission QY up to 35% via hot solution phase chemistry using a nucleation−doping strategy. The PL of the resulting QDs with various shell thicknesses is characterized by steady-state and time-resolved PL spectroscopy to understand the PL mechanism in MnS/ZnS core/shell QDs. A significant enhancement of the PL of Mn^{2+} ions with increasing temperature is demonstrated in the temperature-dependent PL spectra of the core−shell QDs with a thicker shell. We study the PL QY and lifetime of Mn^{2+} ions in the core/shell QDs as a function of the shell thickness to explore the improvement mechanism of the PL QY by the control of the shell thickness.

Experimental Section

A. Sample Preparation. ***1. Materials.*** Zinc stearate ($ZnSt_2$, 12.5−14% ZnO), stearic acid (SA, 95%), and octadecylamine (ODA, 95%) were purchased from Alpha Aesar. 1-Octadecene (ODE) was purchased from Aldrich. Sulfur powders (99.99%) and manganese chloride ($MnCl_2$) were purchased from Shenyang Xinhe Chemical Reagent Company. All chemicals were used without further purification.

2. Synthesis of MnS/ZnS Core/Shell QDs through the Nucleation−Doping Strategy. *a. Preparation of Manganese Stearate.* The manganese precursor, manganese stearate ($MnSt_2$), was prepared according to a method reported in ref 16.

b. Preparation of Stock Solutions. ODES solution was prepared by adding 0.039 g of S to 4 mL of ODE. Several types of zinc precursor solutions were prepared according to the needed MnS/ZnS core/shell QDs with different precursor ratios of Mn/Zn. For example, when the QDs with a precursor ratio of Mn/Zn = 1:13 was needed, the zinc precursor solution was prepared by adding $ZnSt_2$ (0.4 g) and SA (0.04 g) into 3.5 mL of ODE; the total solution was about 4 mL. Similarly, if the QDs with a precursor ratio of Mn/Zn = 1:26 was needed, the zinc precursor solution was prepared by adding $ZnSt_2$ (0.8 g) and SA (0.08 g) into 6 mL of ODE; the total solution was about 7 mL.

c. Typical Synthesis of MnS/ZnS Core/Shell QDs with a Precursor Ratio of Mn/Zn = 1:26. ODE (10 mL) and 0.03 g of $MnSt_2$ were loaded into a 50 mL three-neck flask and degassed at 110 °C for 15 min by bubbling with argon. The temperature was then raised to 270 °C. In a separate vial, ODA (0.4 g) and 4 mL of ODES stock solution were mixed and heated until the solution turned to colorless and then cooled to about 170 °C and injected into the above reaction flask at 270 °C. Immediately after the injection, the color of the solution turned faint yellow, showing the formation of MnS nanoclusters. The reaction was swiftly cooled to 70 °C in order to obtain small, monodispersed MnS QDs and then slowly increased to 250 °C for ZnS overcoating. Next, heated $ZnSt_2$ stock solution in ODE (3 mL) was injected into the reaction flask. Immediately after the injection, the solution started to glow yellow under UV light, which indicated growth of a ZnS shell on MnS cores. The remaining $ZnSt_2$ stock solution was injected by adding 2 mL after 15 min intervals two times. Finally, the reaction was cooled to room temperature, and the QDs were precipitated using acetone.

SCHEME 1: Schematic Structures of the MnS/ZnS QDs Synthesized by the Nucleation−Doping Strategy

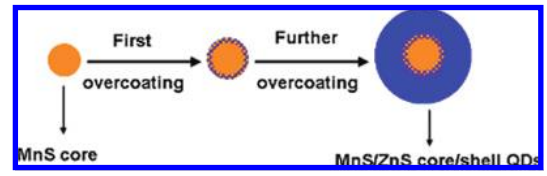

B. Measurements. The morphology and structure of the samples were characterized by transmission electron microscopy (TEM) and high-resolution transmission electron microscopy (HRTEM) (JEOL 2100). In the measurements of fluorescence dynamics, a 266 nm laser generated from a pulsed Nd:YAG (yttrium aluminum garnet) laser combined with a fourth harmonic generator was used as an excitation light with a line width of 0.2 cm^{-1}, a pulse duration of 10 ns, and a repetition frequency of 10 Hz. A Spex 1403 spectrometer and a boxcar integrator were used to record the fluorescence dynamics. In the measurements of temperature-dependent PL, the samples were put into a liquid nitrogen cycling system, in which the temperature varied in the range of 100−300 K. A continuous 325 nm light of a He−Cd laser was used as the excitation source. The fluorescence was measured by a UV-Lab Raman Infinity (made by Jobin Yvon Company) with a spectral resolution of 2 cm^{-1}. In the attempt to calculate the PL QY, a direct measurement of the PL QY by comparing the solution to an organic dye will cause a large error due to the large Stokes shift in the ZnS:Mn QDs. The QY measurement was, therefore, performed by comparing the doped QD solution to a solution of orange-emitting CdSe QDs with the same PL QY of 20% at excitation wavelengths of 320 and 490 nm, previously calibrated to a solution of Rhodamine 6G dye (QY ∼95%).[16] The absorption spectra were recorded on a UV-3101PC UV−vis-NIR scanning spectrophotometer (Shimadzu). Fluorescence and excitation spectra were recorded by a Hitachi F-4500 spectrophotometer equipped with a 150 W Xe arc lamp at room temperature.

Results and Discussion

It is known that the emission properties of Mn^{2+} ions are closely related to the distribution of Mn^{2+} ions in the doped QDs and the structure of the doped QDs. It is necessary to understand their luminescence mechanism by changing the structure of the QDs. Scheme 1 describes the structure of MnS/ZnS core/shell QDs synthesized via the nucleation−doping strategy. First, small-sized MnS cores are formed under the cationic precursor $MnSt_2$ and excess S precursor. Further, during the process of the first overcoating of ZnS shells on MnS cores, an amount of Mn^{2+} ions will diffuse into the ZnS layer, forming a diffusion region. This diffusion is likely more difficult during the further overcoating process due to the relatively deeper placed dopant ions in the QDs.[16,22] Therefore, the diffusion seems to be limited to a relatively thin ZnS shell and the Mn^{2+} ion emission centers should almost be located at the interface between the MnS cores and ZnS shells with high concentration.[16] Therefore, the obtained MnS/ZnS core/shell QDs can be also considered as MnS/ZnS:Mn/ZnS spherical QW QDs.

Figure 1 shows UV−visible absorption, PL, and excitation spectra of MnS/ZnS core/shell QDs with different shell thicknesses prepared with Mn/Zn precursor ratios of 1:6, 1:10, 1:16, and 1:26. As seen in Figure 1, the obtained MnS QDs exhibit a well-resolved $1S_e-1S_h$ excitonic transition peaked at about 278 nm (4.46 eV). The absorption peak is considerably blue

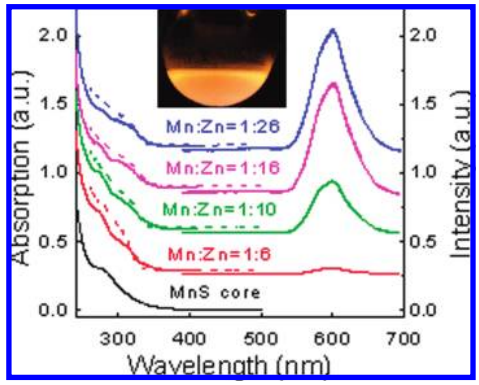

Figure 1. UV−visible (left solid lines), PL (right solid lines), and excitation (left dashed lines) spectra of MnS/ZnS core/shell QDs. The Mn to Zn precursor ratios are given in the figure. The inset shows a digital image taken from a reaction flask in the case of Mn/Zn = 1:26 under a hand-held UV lamp irradiation with the wavelength of 310 nm.

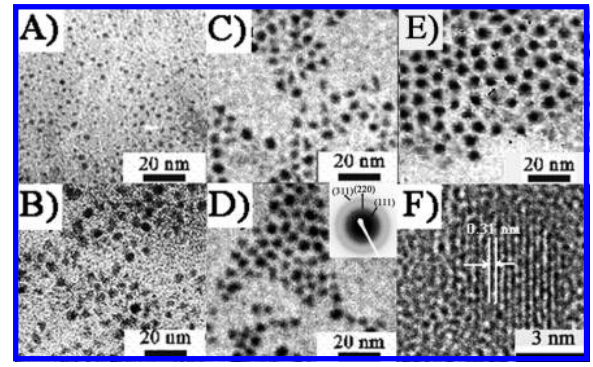

Figure 2. TEM images of MnS cores (A) and MnS/ZnS core/shell QDs with shell thicknesses of 3.1 MLs (B), 4.2 MLs (C), 5.0 MLs (D), and 6.0 MLs (E). Image F shows a typical HRTEM image of a MnS/ZnS core/shell QD with a diameter of 5.4 nm. The representative electron diffraction pattern of the d-dots is illustrated as the inset in image D.

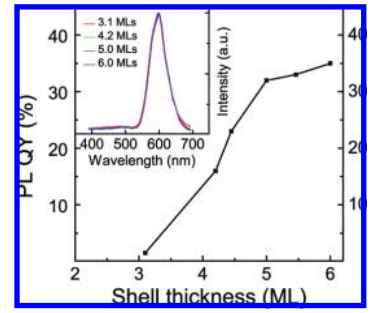

Figure 3. PL QY of MnS/ZnS QDs as a function of the shell thickness. The normalized PL spectra for MnS/ZnS core/shell QDs with different shell thicknesses recorded at room temperature are shown as an inset.

shifted due to the quantum confinement effect, compared with the absorption onset of bulk zinc blend MnS (~3.7 eV).[23] For all MnS/ZnS core/shell samples, the absorption spectra show the characteristics of a QW structure,[16] and the shoulder peaked at about 315 nm is related to the absorption of ZnS shells. On the other hand, a strong PL band is observed at about 597 nm and its intensity rapidly increases with increasing the shell thickness. In general, the orange PL band is considered to originate from a typical emission of Mn^{2+} ions due to its $^4T_1$ to $^6A_1$ transition in a ZnS crystal.[6−8] Besides the strong PL band, a very weak PL band that appears near 400−500 nm comes from the emission of trap states in the ZnS host[5,24,25] and other impurities that are not removed from the resulting QD solution by the purification process, as confirmed in the excitation spectra (not shown here). Compared with that of the previously reported ZnS:Mn d-dots,[5,24,25] the trap state emission is greatly suppressed in our samples, implying preparation of the high-quality Mn-doped QDs. Further, the excitation spectra of the orange emission in the MnS/ZnS core/shell QDs are consistent with the absorption onset of the ZnS shells, indicating that energy transfer comes from the photoexcited ZnS shells to the Mn^{2+} ions.[6−8] In addition, it is noted that the onset in the excitation spectra shifts to the low-energy side with increasing Zn/Mn precursor ratio, suggesting the increase of the ZnS shell thickness.

Typical TEM and high-resolution (HR) TEM images of MnS/ZnS core/shell QDs with different ZnS shell thicknesses are shown in Figure 2. As seen from images A−E in Figure 2, the QDs with a nearly spherical shape become larger with the shell growth. The diameters of the MnS cores and MnS/ZnS QDs were determined to be 2.3 nm and 4.2, 4.9, 5.4, and 6.0 nm when the amount of zinc precursor was taken with Mn/Zn ratios of 1:6, 1:10, 1:16, and 1:26, respectively. The thicknesses of the ZnS shells were estimated to be about 3.1, 4.2, 5.0, and 6.0 monolayers (MLs) based on the thickness of 0.31 nm for a 1 ML ZnS shell,[26] which are in good agreement with the theoretical values estimated from the amount of injected solution with the Mn/Zn ratio of lower than 1:16. However, the shell thickness deviates from the theoretical one of 6.8 MLs when the Mn/Zn ratio is 1:26. This discrepancy may mean that it is difficult to grow a ZnS shell with the thickness of more than 6.0 MLs on the MnS core in the experiment. A typical HRTEM image (Figure 2F) of a MnS/ZnS QD with a diameter of 5.4 nm shows an interplanar spacing of 0.31 nm, corresponding to the (111) planes of zinc blend ZnS (0.312 nm),[17] which is consistent with the result of the electron diffraction pattern (see the inset in Figure 2D). Similar to most of the particles, the HRTEM images of these QDs reveal the single-crystalline nature of the d-dots. In addition, no crystal interface between the MnS core and ZnS shell is observed in the images.

Figure 3 shows the shell thickness dependence of the PL QY of Mn^{2+} ions for the MnS/ZnS QDs with the same MnS cores of about 2.3 nm in diameter. It is found that the PL QY monotonously increases from 1.5% to 35% when the shell thickness changes from 3.1 to 6.0 MLs, indicating the significant improvement of the PL efficiency in the MnS/ZnS QDs by a thick ZnS shell. Similar PL enhancement with increasing shell thickness was also observed in MnSe/ZnSe QDs prepared by the nucleation−doping strategy.[16] However, unlike the obviously size-dependent Mn^{2+} ion emission from ZnSe:Mn QDs,[16] no significant change in the PL line shape and the peak energy is observed in the normalized PL spectra when the shell thickness varies from 3.1 to 6.0 MLs, as shown in the inset of Figure 3. In principle, the peak wavelength of the Mn^{2+} ion emission in Mn-doped groups II−VI semiconductor QDs is mainly determined by the phonon coupling strength and crystal field strength.[27−30] For instance, the Mn^{2+} ion emissions were observed at 591, 588, and 581 nm, respectively, in 10, 4.5, and 3.5 nm sized ZnS:Mn QDs. Phonon coupling was considered as the main reason for the emission shift.[28] Ithurria et al.[30] found that the PL peak varied incrementally from 593 to 632 nm as the ZnS shell increased to 7.5 MLs in Mn^{2+} ions doped in the shell of CdS/ZnS core/shell QDs, which was explained by the change of the local crystal field strength upon Mn^{2+} dopants inside the QDs. According to ref 28, we can consider that the phonon coupling may have little influence on the emission

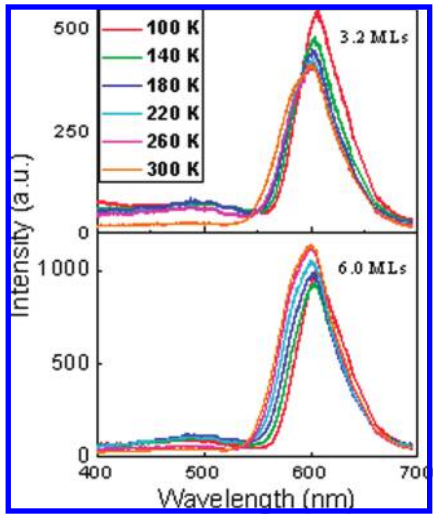

Figure 4. Temperature-dependent PL spectra of MnS/ZnS core/shell QDs with shell thicknesses of 3.1 and 6.0 MLs.

energy of Mn^{2+} ion for the QDs with the size in the range of 4.2 to 6.0 nm in this experiment. Therefore, the weak dependence of the PL peak energy and line shape may mean that the low lattice mismatch between the MnS core and the ZnS shell causes a small change in the local crystal strain in the four samples. It is noted that the peak wavelengths of Mn^{2+} ion emissions in our samples (597 nm) are somewhat redder than that (580−590 nm) in Mn^{2+} homogeneously doped ZnS:Mn d-dots.[17,18] This is likely attributed to a high concentration of Mn^{2+} ions at the interface of MnS cores and ZnS shells.[4,11]

The temperature dependence of the PL spectra for MnS/ZnS core/shell QDs with shell thicknesses of 3.1 and 6.0 MLs is shown in Figure 4. As seen in Figure 4, the PL intensity of the Mn^{2+} ions in the QDs with a shell thickness of 3.1 MLs monotonously decreases with increasing temperature from 100 to 300 K, whereas the PL intensity of the Mn^{2+} ions in the QDs with a shell thickness of 6.0 MLs increases with increasing temperature from 140 to 300 K. Further, the peak wavelength of the PL band shifts to the blue and the full width at half-maximum (fwhm) broadens with increasing temperature.

Figure 5 shows the PL fwhm, peak energy, and intensity of Mn^{2+} ions in MnS/ZnS QDs with different shell thicknesses as a function of temperature. As seen in Figure 5a, the fwhm's of MnS/ZnS QDs with various shell thicknesses show almost the same broadening trend from about 39 nm at a temperature of 100 K to about 50 nm at a temperature of 300 K. The electron−phonon coupling is considered to be responsible for the variation of the emission line width with temperature.[31,32] As seen in Figure 5b, the peak wavelengths of the PL bands in these core/shell QDs blue shift for about 10 nm when the temperature increases from 100 to 300 K. The blue shift of the Mn^{2+} ion emission wavelength with increasing temperature results from crystal lattice contraction at low temperature,[31,33] which is similar to the temperature behavior of Mn^{2+} ion emission in bulk semiconductors.[34] As seen in Figure 5c, the temperature dependence of the PL-integrated intensity clearly varies with the increase of the shell thickness. In contrast to the monotonous decrease of the PL-integrated intensity with increasing temperature observed in the QDs with a 3.1 ML ZnS shell, a significant increase of the PL intensity with increasing temperature in the high-temperature region is found in the QDs with a thick shell. The different temperature dependence of Mn^{2+} ion emissions in Mn-doped groups II−VI semiconductor QDs has been reported by several groups. Su et al.[34] found that the

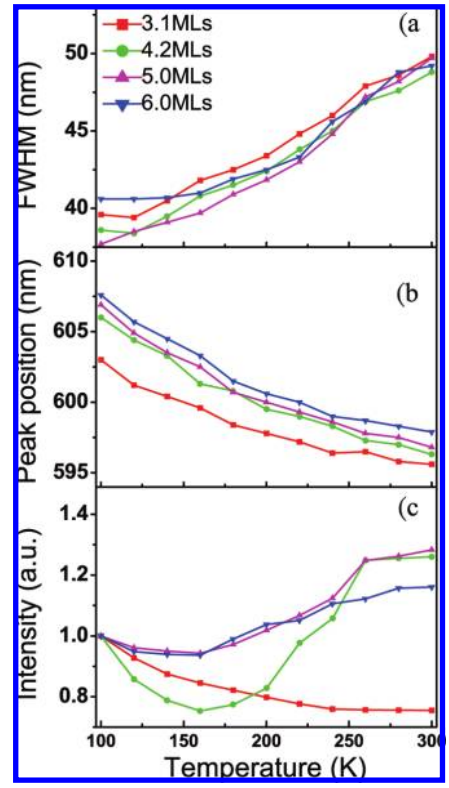

Figure 5. Temperature dependence of the PL fwhm (a), peak energy (b), and integral intensity (c) of Mn^{2+} ions in MnS/ZnS core/shell QDs with different shell thicknesses. The integrated intensity of the Mn^{2+} ion emission in the QDs at different temperatures is normalized to the PL one at the lowest temperature of 100 K.

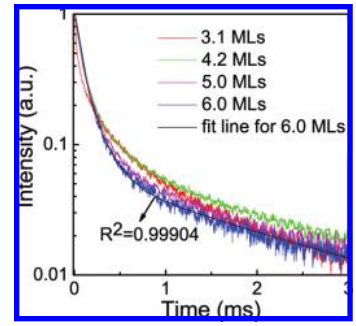

Figure 6. PL decay curves of MnS/ZnS core/shell QDs with different shell thicknesses recorded at room temperature. The black line represents a fit curve of the QDs with a shell thickness of 6.0 MLs.

PL intensity of Mn^{2+} ions in the 3 nm ZnS:Mn QDs increased rapidly from 110 to 300 K, whereas the intensity in the 4.5 nm ZnS:Mn sample was only weakly dependent on temperature. In 2.9 nm ZnSe:Mn QDs, a more than 3-fold decrease in the PL QY was observed when the temperature increased from 50 K to room temperature.[14] Generally, the temperature dependence of the Mn^{2+} ion emission band can be explained by the two competing factors of the thermal quenching in QDs and efficient energy transfer from the delocalized carriers to Mn^{2+} ion emission centers. As shown in Figure 5c, the temperature dependence of the PL intensity for the QDs with a 3.1 ML shell is obviously different from that for the other three samples. This means that there are more nonradiative recombination centers in the former, consistent with the much lower QY than those of the other three samples. When the MnS/ZnS QDs were further overcoated with a thicker shell, the nonradiative recombination centers could be efficiently blocked, suppressing the thermally

TABLE 1: PL QY; Time Constants τ_1, τ_2, and τ_3; the Corresponding Amplitudes of Components A_1%, A_2%, and A_3%; and Average Lifetime τ_{av} of the MnS/ZnS QDs with Different Shell Thicknesses

sample	QY (%)	τ_1 (ms)	A_1%	τ_2 (μs)	A_2%	τ_3 (μs)	A_3%	τ_{av} (ms)
MnS/ZnS (3.1 MLs)	1.5	1.21	7.6	180	31.3	18	61.1	0.83
MnS/ZnS (4.2 MLs)	16	1.82	7.0	186	33.5	53	59.5	1.09
MnS/ZnS (5.0 MLs)	32	1.84	5.6	187	35.9	60	58.5	0.98
MnS/ZnS (6.0 MLs)	35	1.79	5.1	173	35.8	56	59.1	0.95

activated nonradiative relaxation process. Therefore, this indicates that more efficient energy transfer from the delocalized carriers to Mn^{2+} ion emission centers takes place in the QDs with a thicker ZnS shell with increasing temperature.

The PL decay curves of Mn^{2+} ions for the MnS/ZnS QDs with various shell thicknesses are shown in Figure 6. For all four samples, the emissions detected at 597 nm exhibit a nonexponential decay that can be fitted by a triexponential function, $I(t) = y_0 + A_1 \exp(-t/\tau_1) + A_2 \exp(-t/\tau_2) + A_3 \exp(-t/\tau_3)$, where τ_1, τ_2, and τ_3 are the time constants and A_1, A_2, and A_3 are the normalized amplitudes of the components.[35] The average lifetimes τ_{AV} are determined by the expression $\tau_{AV} = (A_1\tau_1^2 + A_2\tau_2^2 + A_3\tau_3^2)/(A_1\tau_1 + A_2\tau_2 + A_3\tau_3)$.[36] The time constants and the PL QYs of the MnS/ZnS QDs are summarized in Table 1. From Table 1, we can see that the decay time constants of the three components are on the scale of 1−2 ms, hundreds of μs, and tens of μs, respectively. The slowest (1.2−1.8 ms) and medium (144−196 μs) ones are attributed to the emission of the single isolated Mn^{2+} ions in a cubic site[7,8] and the exchange coupled Mn^{2+} ion pairs,[11] respectively. The fastest decay component with the time constants of 15−60 μs might have some contributions from nonradiative decay or be related to the emission of the Mn^{2+} ions with enhanced overlap between 3d and sp host states caused by lattice strain due to the particular distributions of Mn^{2+} ions in the ZnS:Mn d-dots.[12]

Interestingly, it is noted in Table 1 that the shell thickness dependence of the PL QY is obviously different from that of the average PL lifetime. With the growth of the ZnS shell thickness from 3.1 to 6.0 MLs on the MnS core, the PL QY increases monotonously from 1.5% to 35% while the average PL lifetime almost keeps unchanged despite a slight increase from 0.83 to 1.09 ms when the shell thickness increases from 3.1 to 4.2 MLs. Similarly, a slight increase in the PL lifetime from 1.70 to 1.74 ms was reported in coated ZnS:Mn dots with a ZnS shell, whereas the integrated PL intensity was found to increase by 30%.[17] To understand the difference between the variations of the PL intensity and lifetime with the shell thickness in MnS/ZnS QDs, a schematic diagram of the relaxation dynamic process is shown in Figure 7.

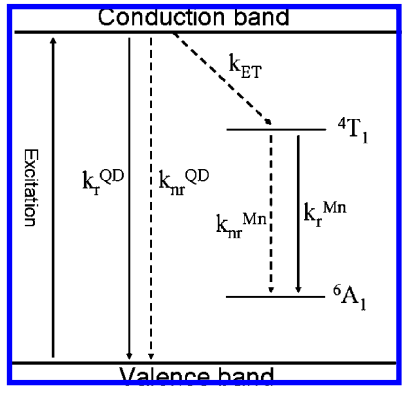

Figure 7. Schematic of energy levels induced by Mn^{2+} ions in MnS/ZnS core/shell QDs and the corresponding kinetic parameters. k_r and k_{nr} are linear decay rates for radiative and nonradiative processes, and k_{ET} describes the rate of nonradiative energy transfer from the QD to the Mn^{2+} ions.

Under the conditions of steady-state excitation, the PL lifetime of the Mn^{2+} ion emission, τ^{Mn}; the efficiency of the energy transfer from the QDs to Mn^{2+} ions, Φ_{ET}; the efficiency of the Mn^{2+} ion emission, Φ_{Mn}; and the PL QY of Mn^{2+} ions, QY^{Mn}, can be expressed by eqs 1−4[26]

$$1/\tau^{Mn} = k_r^{Mn} + k_{nr}^{Mn} \quad (1)$$

$$\Phi_{ET} = k_{ET}/(k_{nr}^{QD} + k_r^{QD} + k_{ET}) \quad (2)$$

$$\Phi_{Mn} = k_r^{Mn}/(k_r^{Mn} + k_{nr}^{Mn}) \quad (3)$$

$$QY^{Mn} = \Phi_{ET} * \Phi_{Mn} \quad (4)$$

where k_r^{Mn} and k_{nr}^{Mn} are the intrinsic radiative and nonradiative decay rates of the excited state of Mn^{2+} ions, respectively. k_{ET} is the phenomenological rate of energy transfer from the QD to the ensemble of Mn^{2+} ions within the QD and is dependent on the concentration and spatial distribution of Mn^{2+} ions inside the QD,[37] k_r^{QD} is the radiative decay rate of the QD, and k_{nr}^{QD} is the sum of all nonradiative decay rates of the QD not involving the dopants.

In this experiment, the change of k_r^{Mn} in our four samples can be ignored because the increase of the shell thickness to about 3 MLs cannot affect much the wave function properties of the $^4T_1$ and $^6A_1$ states of the Mn^{2+} ion.[26] In addition, the increase of the shell thickness should not change the numbers and spatial distribution of Mn^{2+} ions at the MnS/ZnS interface; therefore, the change of k_{ET} in our four samples can be ignored. Further, k_r^{QD} can be set to zero because of a very weak emission from the ZnS host even at low temperature.

Combined with eqs 1 and 3, eq 4 can be rewritten as

$$QY^{Mn} = \Phi_{ET} * k_r^{Mn} * \tau^{Mn} \quad (5)$$

From eq 5, we can see that the PL QY of Mn ions is determined not only by the PL lifetime of Mn^{2+} ions (τ^{Mn}) but also by the efficiency of the energy transfer (Φ_{ET}) from an exciton inside the ZnS shell to Mn^{2+} ions. Indeed, the difference between the ZnS:Mn d-dots and undoped (such as pure CdSe) QDs is that the Mn^{2+} ion emission in ZnS:Mn d-dots comes from the energy transfer from the ZnS host to the Mn^{2+} ions not from direct excitation like PL in CdSe QDs. The PL lifetimes of Mn^{2+} ions in the MnS/ZnS QDs are found to be weakly dependent on the shell thickness, as seen in Table 1, which can be easily understood based on the surface-quenching model proposed in ref 38. According to eq 5, we can reasonably understand the mechanism for the improvement of the PL QY. That is, the surface passivation of ZnS:Mn d-dots by the growth of a thick ZnS shell on the MnS core significantly reduces the

nonradiative relaxation rate of the QDs (k_{nr}^{QD}) to increase the efficiency of the energy transfer from the ZnS shell to Mn^{2+} ions (Φ_{ET}) and slightly decreases the nonradiative relaxation rate (k_{nr}^{Mn}) from the Mn^{2+} ions at the core/shell interface to the surface-quenching centers to increase the PL lifetime of Mn^{2+} ions in QDs with a thicker shell.[38]

Conclusions

In summary, we have synthesized highly efficient luminescent MnS/ZnS core/shell QDs using the nucleation−doping strategy. It is found that the PL QY of Mn^{2+} ions could reach 35% despite a high concentration of Mn^{2+} ions at the MnS/ZnS interface, which is much higher than that of the QDs synthesized by traditional methods. The experimental results indicate that the more efficient energy transfer from the ZnS host to Mn^{2+} ion emission centers (Φ_{ET}) results in the enhancement of the PL QY in the core/shell QDs with a thicker shell by decreasing the nonradiative decay rate of the host. On the other hand, the highly efficient PL might also result from the structure of a spherical QW, preventing the concentration quenching of the Mn^{2+} ions by controlling the energy transfer process in two-dimensional planes. Therefore, it is expected to synthesize high-quality Mn-doped groups II−VI semiconductor QDs via the special control of the QD structure.

Acknowledgment. This work was supported by the program of CAS Hundred Talents, the NSF of China (10874179, 10674132, and 60771051), and the Pre-Strategic Initiative of University of Tsukuba, Japan.

References and Notes

(1) Wood, V.; Halpert, J. E.; Panzer, M. J.; Bawendi, M. G.; Vladimir, B. *Nano Lett.* **2009**, *9*, 2367.
(2) Yang, H.; Holloway, P. H.; Ratna, B. B. *J. Appl. Phys.* **2003**, *93*, 586.
(3) Zhuang, J. Q.; Zhang, X. D.; Wang, G.; Li, D. M.; Yang, W. S.; Li, T. J. *J. Mater. Chem.* **2003**, *13*, 1853.
(4) Thakar, R.; Chen, Y. C.; Snee, P. T. *Nano Lett.* **2007**, *7*, 3429.
(5) Becker, W. G.; Bard, A. J. *J. Phys. Chem.* **1983**, *87*, 4888.
(6) Bhargava, R. N.; Gallagher, D.; Hong, X.; Nurmikko, A. *Phys. Rev. Lett.* **1994**, *72*, 416.
(7) Bol, A. A.; Meijerink, A. *Phys. Rev. B* **1998**, *58*, R15997.
(8) Smith, B. A.; Zhang, J. Z.; Joly, A.; Liu, J. *Phys. Rev. B* **2000**, *62*, 2021.
(9) Chen, L.; Zhang, J. H.; Luo, Y. S.; Lu, S. Z.; Wang, X. J. *Appl. Phys. Lett.* **2004**, *84*, 112.
(10) Mee, R. K.; Jae, H. Ch.; Du-Jeon, J. *Phys. Chem. Chem. Phys.* **2009**, *11*, 1003.
(11) Qian, L.; Bera, D.; Holloway, P. *Appl. Phys. Lett.* **2008**, *92*, 093103.
(12) Park, W.; Jones, T. C.; Tong, W.; Schon, S.; Chaichimansour, M.; Wagner, B. K.; Summers, C. J. *J. Appl. Phys.* **1998**, *84*, 6852.
(13) Erwin, S. C.; Zu, L.; Haftel, M. I.; Efros, A. L.; Kennedy, T. A.; Norris, D. J. *Nature* **2005**, *436*, 91.
(14) Norris, D. J.; Yao, N.; Charnock, F. T.; Kennedy, T. A. *Nano Lett.* **2001**, *1*, 3.
(15) Mikulec, F. V.; Kuno, M.; Bennati, M.; Hall, D. A.; Griffin, R. G.; Bawendi, M. G. *J. Am. Chem. Soc.* **2000**, *122*, 2532.
(16) Pradhan, N.; Peng, X. *J. Am. Chem. Soc.* **2007**, *129*, 3339.
(17) Quan, Z. W.; Wang, Z. L.; Yang, P. P.; Lin, J.; Fang, J. Y. *Inorg. Chem.* **2007**, *46*, 1354.
(18) Cao, L. X.; Zhang, J. H.; Ren, S. L.; Huang, S. H. *Appl. Phys. Lett.* **2002**, *80*, 4300.
(19) Karar, N.; Chander, H.; Shivaprasad, S. M. *Appl. Phys. Lett.* **2004**, *85*, 5058.
(20) Peng, X. G.; Schlamp, M. C.; Kadavanich, A. V.; Alivisatos, A. P. *J. Am. Chem. Soc.* **1997**, *119*, 7019.
(21) Yang, H.; Holloway, P. H. *Adv. Funct. Mater.* **2004**, *14*, 152.
(22) Chen, D. G.; Viswanatha, R. J.; Ong, G. L.; Xie, R. G.; Balasubramaninan, M.; Peng, X. G. *J. Am. Chem. Soc.* **2009**, *131*, 9333.
(23) Zheng, Y. H.; Cheng, Y.; Wang, Y. S.; Zhou, L. H.; Bao, F.; Jia, C. *J. Phys. Chem. B* **2006**, *110*, 8284.
(24) Denzier, D.; Olschewski, M.; Sattler, K. *J. Appl. Phys.* **1998**, *84*, 2841.
(25) Sooklal, K.; Cullum, B. S.; Angel, S. M.; Murphy, C. J. *J. Phys. Chem.* **1996**, *100*, 4551.
(26) Yang, Y. G.; Chen, O.; Angerhofer, A.; Cao, Y. *Chem.—Eur. J.* **2009**, *15*, 3186.
(27) Tanaka, M.; Qi, J.; Masumoto, Y. *J. Lumin.* **2000**, *87*, 472.
(28) Chen, W.; Sammynaiken, R.; Huang, Y. N.; Malm, J. O.; Wallenberg, R.; Bovin, J. O.; Zwiller, V.; Kotov, N. A. *J. Appl. Phys.* **2001**, *89*, 1120.
(29) Nirmal, M.; Murray, C. B.; Norris, D. J.; Bawendi, M. G. *Z. Phys. D* **1993**, *26*, 361.
(30) Ithurria, S.; Guyot-Sionnest, P.; Mahler, B.; Dubertret, B. *Phys. Rev. Lett.* **2007**, *99*, 265501.
(31) Chen, W.; Su, F.; Li, G.; Joly, A. G.; Malm, J.-O.; Bovin, J.-O. *J. Appl. Phys.* **2002**, *92*, 1950.
(32) Huang, K. *Prog. Phys.* **1981**, *1*, 31.
(33) Chen, W.; Aguekian, V. F.; Vassiliev, N.; Serov, A. Y.; Filosofov, N. G. *J. Chem. Phys.* **2005**, *123*, 124707.
(34) Su, F. H.; Ma, B. S.; Fan, Z. L.; Ding, K.; Li, G. H.; Chen, W. *J. Phys.: Condens. Matter* **2002**, *14*, 12657.
(35) Morello, G.; Anni, M.; Cozzoli, P. D.; Manna, L.; Cingolani, R.; Giorgi, M. D. *J. Phys. Chem. C* **2007**, *111*, 10541.
(36) Zhang, Y. L.; Jing, P. T.; Zeng, Q. H.; Sun, Y. J.; Su, H. P.; Wang, Y. A.; Kong, X. G.; Zhao, J. L.; Zhang, H. *J. Phys. Chem. C* **2009**, *113*, 1886.
(37) Beaulac, R.; Archer, P. I.; Ochsenbein, S. T.; Gamelin, D. R. *Adv. Funct. Mater.* **2008**, *18*, 3873.
(38) Gao, C. C.; Huang, S. H.; You, F. T.; Kang, K.; Feng, Y. *Chin. Phys. Lett.* **2008**, *25*, 698.

JP906390Y